Control of tipping points in stochastic mutualistic complex networks

Cite as: Chaos **31**, 023118 (2021); https://doi.org/10.1063/5.0036051
Submitted: 03 November 2020 . Accepted: 26 January 2021 . Published Online: 10 February 2021

Yu Meng, and Celso Grebogi

Control of tipping points in stochastic mutualistic complex networks

Cite as: Chaos **31**, 023118 (2021); doi: 10.1063/5.0036051
Submitted: 3 November 2020 · Accepted: 26 January 2021 ·
Published Online: 10 February 2021

View Online Export Citation CrossMark

Yu Meng[a] and Celso Grebogi

AFFILIATIONS

Institute for Complex Systems and Mathematical Biology, King's College, University of Aberdeen, Aberdeen AB24 3UE, United Kingdom

[a]**Author to whom correspondence should be addressed:** r02ym17@abdn.ac.uk

ABSTRACT

Nonlinear stochastic complex networks in ecological systems can exhibit tipping points. They can signify extinction from a survival state and, conversely, a recovery transition from extinction to survival. We investigate a control method that delays the extinction and advances the recovery by controlling the decay rate of pollinators of diverse rankings in a pollinators–plants stochastic mutualistic complex network. Our investigation is grounded on empirical networks occurring in natural habitats. We also address how the control method is affected by both environmental and demographic noises. By comparing the empirical network with the random and scale-free networks, we also study the influence of the topological structure on the control effect. Finally, we carry out a theoretical analysis using a reduced dimensional model. A remarkable result of this work is that the introduction of pollinator species in the habitat, which is immune to environmental deterioration and that is in mutualistic relationship with the collapsed ones, definitely helps in promoting the recovery. This has implications for managing ecological systems.

Ecologically complex networks can exhibit a tipping point due to deteriorating conditions for species survival. It represents an extreme decline in abundance of species in a habitat. A number of random perturbations in actual ecological networks, such as demographic noise due to dynamic changes within populations and environmental noise due to external environmental disturbances, have a major effect in the tipping point dynamics. We propose a method to control the tipping point in pollinators–plants networks by controlling the decay rate of selected pollinator species. In this work, we show that the control delays the onset of the tipping point collapse, and, additionally, it advances the recovery of species after the collapse. Our results are highly relevant for ecological habitat management.

I. INTRODUCTION

Control is a timely and fundamental research topic in complex systems,[1–9] including applications in power systems,[9] engineering systems,[10] health systems,[11] and ecosystems.[1] Exploring its general theory in a quantitative way to control a weighted, directed network is one of the most frequently encountered problems in physical systems,[1,12,13] and methods for solving the controllability[3,4] of arbitrary network topologies and sizes have been extensively investigated. In ecosystem studies, the state of species within an effective control system is important for habitat management. Control of real ecosystems is often plagued by nonlinearity, high dimensionality, and stochasticity,[14–24] the latter both intrinsic to species populations and caused by external environmental perturbations. In this work, we investigate control methods in high-dimensional nonlinear stochastic complex ecosystems. In particular, we study the effectiveness of controlling tipping points in ecosystems when subjected to both environmental and demographic stochasticities.[14,20,21,24] We also address the effect of network structure on control effectiveness.

The mutualistic coexistence network of pollinators and plants is the ecosystem addressed in this work. A mutualistic relationship, often encountered in nature, is a close relationship between two organisms of different species, where each species benefits from the interaction with the other.[25–29] A tipping point may occur in a mutualistic system; it denotes a transition from a survival state to an extinction state as a system parameter changes past the collapse tipping point.[28–40] There is also a recovery tipping point in a system when the system parameter is reversed passing the tipping point from an extinction to survival state. There are many reasons for the change in system parameters, such as environmental degradation due to climate change,[41] competition within the system between

species, species reproduction and depopulation, and habitat loss due to agricultural and urban developments.[42,43]

In this work, we propose a practical and effective control method as external intervention to influence the ecosystem. We require that one or more particular pollinators have their species abundances kept at a certain survival state when environmental parameters are altered,[2] i.e., requiring the decay rate of these pollinators to be zero. Due to mutualism, the abundances of the controlled species affect the other species, achieving the goal of controlling the entire mutualistic network. According to our simulations, including stochastic effects, controlling the abundance of individual or multiple species can delay the onset of the collapse tipping point, while also allowing for an earlier recovery. By analyzing the control of empirical, random, and scale-free networks with this control method, we find that the control effect is also affected by the structure of the network, depending on the ranking or degree of the individual species being controlled. In addition, based on the previous work,[14,24] noise can change the dynamic behavior of the system. For instance, noise perturbations can contribute for the system to make the transition from the survival to the extinction state. We thus consider noise as one of the influencing factors and discuss the strategies that should be used to determine the control tipping point of a system under noise perturbations. We, therefore, combine noise with control to explore the quantitative relationship between control of species having specific rankings and noise perturbations.

The structure of the paper is as follows. In Sec. II, we present models of stochastic mutualistic networks, the types and empirical data for simulation calculations and control methods, and provide quantitative definitions for measuring control effects and network structure. In Sec. III, we present the control effects of controlling empirical, random, and scale-free networks under noise perturbations during collapse and recovery processes. In Sec. IV, we provide a theoretical analysis and understanding of the tipping point transition mechanism. In Sec. V, we conduct the discussion and conclusions.

II. MODEL AND CONTROL

The mutualistic ecologically complex network we study in this work can be modeled as a bipartite high-dimensional ODE model, with each subset representing pollinators and plants, respectively. The interactions are described by the Holling type II model.[31,32] We numerically simulate the complex network with data from four real-world empirical networks. In order to analyze how the structure affects the control, simulations are also performed with random and scale-free networks to discuss the effect of nestedness and links probability on the control of tipping points in different networks.

We introduce two important quantitative concepts, "control effect" and "mutualistic number," to quantify the control effectiveness and the network structure. Since the system parameter that we vary is the decay rate κ, we define the control effect of the collapse process as $\Delta\kappa = \kappa_c^{control} - \kappa_c$, where $\kappa_c^{control}$ is the value of the tipping point at which one or more pollinators are controlled and κ_c is the collapse tipping point without control. The control effect of the recovery process is $\Delta\kappa = \kappa_r - \kappa_r^{control}$, where $\kappa_r^{control}$ is the recovery point of the controlled pollinators and κ_r is the recovery tipping point without control. Mutualistic number L is the ranking of either a pollinator or a plant in the mutualistic networks.

A. Model of stochastic mutualistic networks

The deterministic mutualistic complex network has been studied mathematically.[27–29,40] We consider mutualistic complex networks under perturbations by environmental noise and demographic noise,[24] which can be modeled as[14]

$$\frac{dX_i}{dt} = \alpha_i^{(X)} X_i - \kappa_i^{(X)} X_i - \sum_{j=1}^{S_X} \beta_{ij}^{(X)} X_i X_j + \frac{\sum_{k=1}^{S_Y} \gamma_{ik}^{(X)} Y_k}{1 + h\sum_{k=1}^{S_Y} \gamma_{ik}^{(X)} Y_k} X_i + \mu_X + \sqrt{N(X_i)}\, dB_i(t), \quad (1)$$

$$\frac{dY_i}{dt} = \alpha_i^{(Y)} Y_i - \sum_{j=1}^{S_Y} \beta_{ij}^{(Y)} Y_i Y_j + \frac{\sum_{k=1}^{S_X} \gamma_{ik}^{(Y)} X_k}{1 + h\sum_{k=1}^{S_X} \gamma_{ik}^{(Y)} X_k} Y_i + \mu_Y + \sqrt{N(Y_i)}\, dB_i(t), \quad (2)$$

where X_i and Y_i are the abundances of the ith pollinator and the ith plant, respectively. S_X and S_Y are numbers of pollinators and plants, respectively. $\alpha_i^{(X)}$ and $\alpha_i^{(Y)}$ are the intrinsic growth rates, β_{ii} and β_{ij} $(i \neq j)$ are parameters characterizing intraspecific and interspecific competition, respectively, and the parameters $\mu_X \gtrsim 0$ and $\mu_Y \gtrsim 0$ characterize species migration. For the pollinator–plant system, intraspecific competition is typically stronger than interspecific competition: $\beta_{ii} \gg \beta_{ij}$.[29] The saturation effect is quantified by the half-saturation constant h of the Holling type II functional response.[32] The terms that involve the mutualistic interactions for each species can then be written as[29] $\sum_{j=1}^{S_Y} \gamma_{ij}^{(X)} Y_j = \sum_{j=1}^{S_Y} \frac{\gamma}{(K_i^{(X)})^\rho} a_{ij} Y_j$ and $\sum_{j=1}^{S_X} \gamma_{ij}^{(Y)} X_j = \sum_{j=1}^{S_X} \frac{\gamma}{(K_i^{(Y)})^\rho} a_{ij} X_j$. The $\gamma_{ik}^{(X)}$ and $\gamma_{ik}^{(Y)}$ are the strengths of the mutualistic interactions that depends on the degree of the node as $\gamma_{ij} = a_{ij} \frac{\gamma}{(N_i)^\rho}$,[29] where γ is the normalized strength and a_{ij}'s are the elements of the network adjacency matrix. The network adjacency matrix is normalized as $a_{ij} = 1$ if there is an interaction between pollinator i and plant j; otherwise, $a_{ij} = 0$. N_i is the number of mutualistic links associated with species i. ρ quantifies the trade-off between the interaction strength and the number of interactions. If there is no trade-off (i.e., $\rho = 0$), the network topology has no effect on the strength of the mutualistic interactions. In contrast, a full trade-off ($\rho = 1$) means that the interaction strength is weighed by the nodal degree so that the network topology affects the species gain from the interactions. $\kappa_i^{(X)}$ is the key parameter we consider for controlling both tipping points, the collapse and recovery processes, and it represents the rate of species decay due to, for example, environmental degradation and other disturbances.

The two noise perturbations are understood as follows. $dB_i(t)$ is Gaussian noise with a normal distribution with zero mean and variance dt. For the effect of environmental noise,

$$N(X_i) = \sigma^2 \quad \text{and} \quad N(Y_i) = \sigma^2, \quad (3)$$

where σ is the noise strength of environmental white noise. Demographic noise depends on the state variables and is modeled as

$$N(X_i) = \xi^2 X_i \quad \text{and} \quad N(Y_i) = \xi^2 Y_i, \tag{4}$$

where the noise strength is ξ. The algorithm for simulating the stochastic equations is in Appendix B of the supplementary material.

In order to study and compare the control effects of different networks and to analyze how the structure affects the control, we perform simulation calculations on four empirical networks, three random networks, and two scale-free networks. The empirical network A ($S_X = 61$ and $S_Y = 17$ with the number of mutualistic links $L = 146$) from empirical data from Hicking, Norfolk, UK; network B ($S_X = 42$, $S_Y = 8$, and $L = 794$) from Hestehaven, Denmark; network C ($S_X = 38$, $S_Y = 11$, and $L = 106$) from Tenerife, Canary Islands, Spain; and network D ($S_X = 44$, $S_Y = 13$, and $L = 143$) from North Carolina, USA.

Nestedness is a measure of structure in an ecosystem[28] that describes the interactions between species in a mutualistic network. By systematically varying the nestedness of the networks, we generate random and scale-free mutualistic networks by rearranging the mutualistic interactions between each species until the desired nestedness value is reached.[14,44] To be specific, we first randomly select an edge, such as the connection between species i and j, and then randomly select another species k. If i is a pollinator, then j and k must be plants and vice versa. If species k has more mutualistic connections than species j, we connect species i and k; otherwise, we do not change the interactions between i and j. Finally, the nestedness of the mutualistic network is denoted as[14]

$$Nest = \frac{\sum_{i<j}^{S_X} D_{ij}^X + \sum_{i<j}^{S_Y} D_{ij}^Y}{S_X(S_X-1)/2 + S_Y(S_Y-1)/2}, \tag{5}$$

where $D_{ij}^X = \frac{d_{ij}^X}{min(d_i^X, d_j^X)}$ and $D_{ij}^Y = \frac{d_{ij}^Y}{min(d_i^Y, d_j^Y)}$, d_{ij}^X represent the numbers of plants that have a mutualistic interaction with both pollinators i and j. d_i^X and d_i^Y are the total numbers of plants species that have a mutualistic interaction with pollinators i and j, respectively. The three random networks we construct in this work have 25 pollinators and 25 plants with nestedness of 0.3, 0.5, and 0.7.

Links probability refers to the distribution of the number of mutualistic links among species. Based on the growth network model, we generate scale-free mutual networks. The network initially has n_0 species, two of which are coupled. A new species is added every unit of time afterward. The new species selects $n \le n_0$ species from the current network to connect to it, and the probability p_i that a species i is selected as a mutualistic interaction partner is proportional to the size of its degree d_i, shown as

$$p_i = \frac{d_i}{\sum_j d_j}. \tag{6}$$

The two scale-free networks have 25 pollinators and 25 plants with *links probabilities* of 0.4 and 0.8.

B. Control method

The control method we use is to control single and multiple pollinators we impose that the environmental decay of these controlled pollinators is zero; i.e., $\kappa_i = 0$. An alternative control method for this ecosystem would require a constant abundance of single or multiple pollinators, but its practical feasibility in a habitat is questionable.

In order to address the control effect with different controlled species, we use the *importance* of control effect to mean the statistical property of the importance of nodes when carrying out the control of the nonlinear dynamical network.[2] The collapse tipping point of the network occurs under the condition that the abundance of species in the network decreases to the extinction state when the decay rate of species κ continues to increase and crosses its tipping point κ_c; i.e., X and Y approach zero when $\kappa \ge \kappa_c$. Conversely, when the value of κ decreases continuously to the recovery point κ_r, the abundance of species in the network returns to the survival state; i.e., the values of X and Y are within a stable positive value range for $\kappa \le \kappa_r$. We show that the value of the collapse point value of κ is greater than κ_c and the value of recovery point κ is less than the value of the original recovery point κ_r when applying control to the network. Control delays the collapse of the system and also advance the recovery of the species.

III. CONTROL EFFECTS FOR COLLAPSE AND RECOVERY PROCESSES

A. Dependence on the ranking and number of pollinators being controlled

As described in Sec. II, we use the method of controlling the decay rate of one or more pollinators to influence the collapse and recovery tipping points. The method is based on selecting pollinators in the survival basin, setting their decay rates to be zero both for the collapse and recovery processes. Since pollinators have different mutualistic interactions in each network and controlling different pollinators have different control effects, we first rank the pollinators according to their mutualistic numbers L. The pollinator with the largest mutualistic numbers is ranked 1, and the remaining pollinators are ranked in a descending order with the number of mutualistic interactions they have. The greater the value of $\Delta\kappa$, the more effective is the control.

The evolution of system collapse is such that as the value of κ increases, the system has a transition from a high-abundance steady state (survival) to a low-abundance steady state (extinction), indicating the occurrence of a tipping point. Figures 1(a)–1(d) shows the collapse of the system when subjected to environmental noise. By comparing the tipping point $\kappa_2 \approx 2$ (red curves) when the controlled system collapses with the tipping point $\kappa_1 \approx 1.75$ (blue curves) when the uncontrolled system collapses, the collapse of the controlled system is significantly delayed. The value of the tipping point is larger in the controlled system, the system being relatively more resilient. In Fig. 1(a), pollinator 1 is controlled, while in Fig. 1(b), pollinator 5 is controlled. By comparing the difference between the red curves in Figs. 1(a) and 1(b), the larger the mutualistic number, or higher ranking, the controlled species has, it results in a better control effect. In Fig. 1(c), pollinators 1 and 7 are controlled. By comparing with Fig. 1(a), controlling multiple species is better than controlling a single species; the more species that are controlled the better is the control effect, as seen by comparing Figs. 1(c) and 1(d). Therefore, the control effect depends on both the ranking and the number

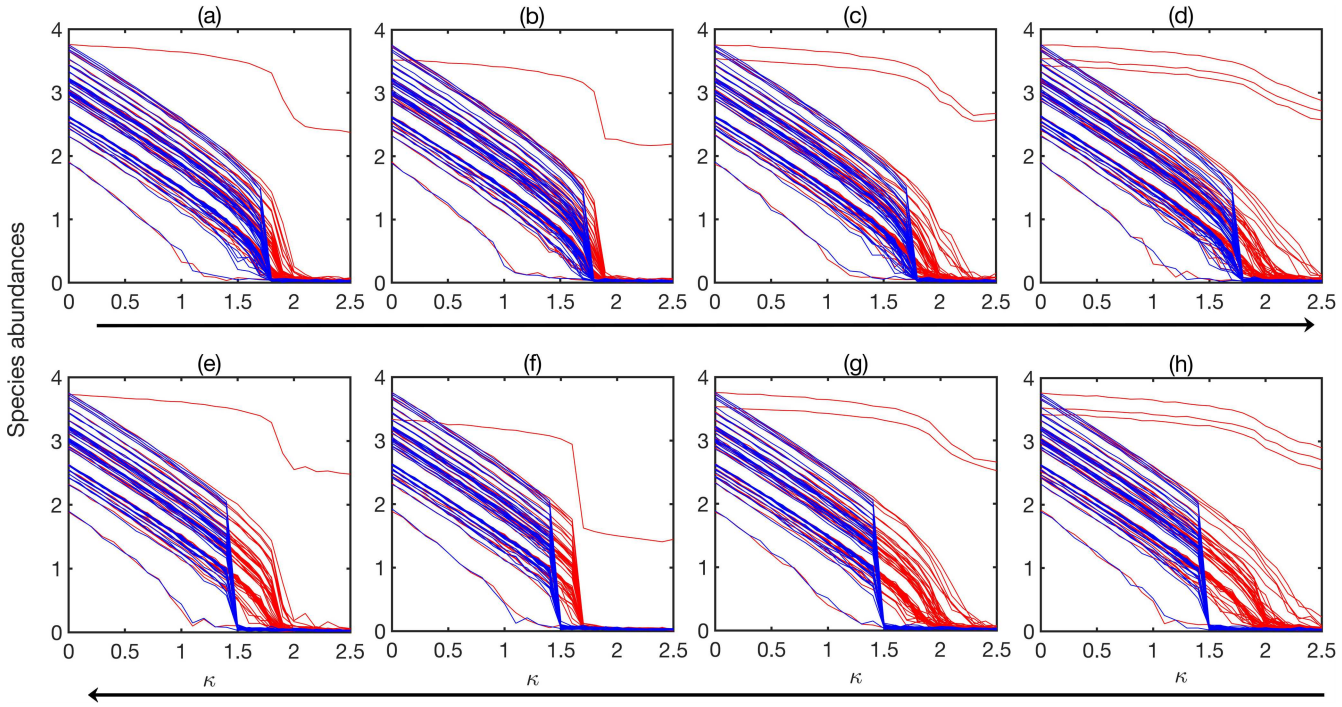

FIG. 1. Controlled collapse and recovery processes with environmental noise for empirical network A. (a)–(d) are the collapse process with additive environmental noise, and (e)–(h) are the recovery process with additive environmental noise. The blue curves are the pollinators' abundances of the recovery process without control and the red curves are the pollinators' abundances when controlling species 1, 5, combination of controlling 1 and 7, and combination of controlling 1, 7, and 20, respectively. The parameters are set as $\alpha^{(X)} = \alpha^{(Y)=0.3}$, $\beta_{ii}^{(X)} = \beta_{ii}^{(Y)} = 1$, $\gamma = 1$, $h = 0.2$, $\rho = 0.5$, and $\mu_X = \mu_Y = 10^{-4}$. The noise strength is $\sigma = 0.1$.

of the pollinators being controlled. Figure 2 is analogous to Fig. 1, but it shows the system perturbed by demographic noise. The control effect is again related to the ranking and number of controlled pollinators. Figures 1(e)–1(h) and 2(e)–2(h) represent the recovery process for the system affected by environmental noise and demographic noise, respectively. The factors influencing the control effect are the same in the recovery process as in the collapse process. The greater the number of mutualistic links L possessed by the controlling pollinators, the better the control effect is, which means that the recovery process of species abundances can be advanced with control. Furthermore, the effect of controlling multiple species is more pronounced than that of controlling a single species. As shown in Fig. 3, the higher is the number of mutualistic interactions of the controlled pollinators, the more effective is the control effect, regardless of the type of noise to which the system is affected.

Comparing Figs. 1(a)–1(d) and 1(e)–1(h) the two tipping points for the system collapse and recovery without control, they do not have the same value, resulting in a hysteresis. It means that when species decay rates are not controlled, the value of κ required for a full recovery is considerably less than the κ value at the collapse tipping point, implying that the environment needs to be considerably better than it was before the collapse in order for pollinator abundances to recover. Importantly, abundance management and control eliminate the hysteresis effect. According to Figs. 1(a)–1(d) and 1(e)–1(h), after the system is controlled, the recovery of species abundance is at the same κ as the tipping point for the collapse.

A remarkable and important consequence of our work, as depicted in Figs. 1(e)–1(h) and 2(e)–2(h), is that the introduction of pollinator species in the habitat, which are in a mutualistic relationship with the collapsed ones, definitely helps by promoting the recovery. This is an important habitat management result coming out of this work.

B. Control effects at different strengths of noise perturbations

According to previous studies,[14,24] noise perturbations change the tipping points for the system collapse and recovery, and different strengths of noise can also cause a change of the tipping points, which means that the conditions for advancing the system's recovery point are different under different noise strengths. Therefore, we discuss next the different control effects when the system is affected by different noises.

We simulate environmental noise in the stochastic networks at noise strengths of 0.1 and 0.001 and find that there is a positive correlation between the control effect and the number of mutualistic links of the controlled pollinators for both environmental noise strengths. Although the noise strength does not change the positive correlation, it changes the control effect $\Delta\kappa$. Figures 3(a) and 3(b)

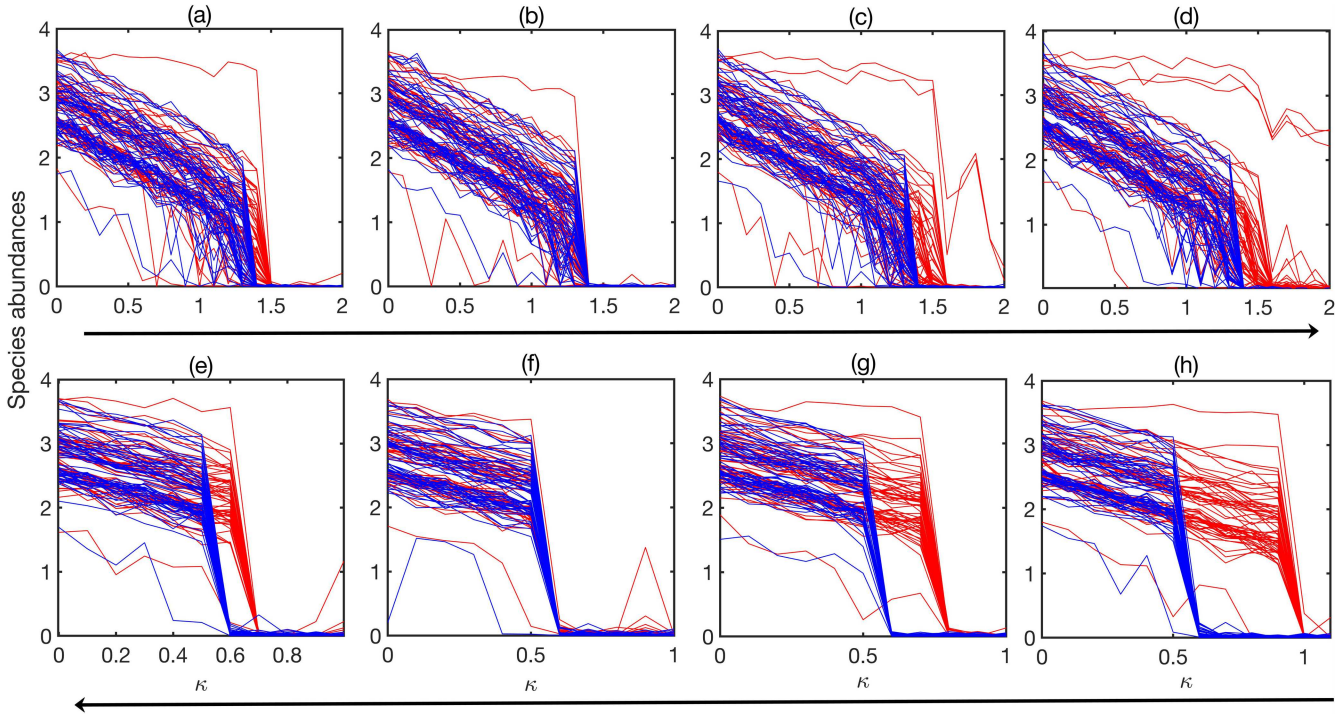

FIG. 2. Controlled collapse and recovery processes with demographic noise for empirical network A. (a)–(d) are the collapse process with demographic noise. (e)–(h) are the recovery process with demographic noise. The blue curves are the pollinators' abundances of the collapse process without control and the red curves are the pollinators' abundances when controlling species 1, 5, combination of controlling 1 and 7, and combination of controlling 1, 7 and 20, respectively. The parameters are set as $\alpha^{(X)} = \alpha^{(Y)=0.3}$, $\beta_{ii}^{(X)} = \beta_{ii}^{(Y)} = 1$, $\gamma = 1$, $h = 0.2$, $\rho = 0.5$, and $\mu_X = \mu_Y = 10^{-4}$. The noise strength is $R = 4$ and $\xi = 1$.

show that the control effect is more pronounced at higher noise strengths. This correlation remains when the system is disturbed by demographic noise, as shown in Figs. 3(c) and 3(d). Interestingly, for the stochastic network, the higher the environmental noise [Figs. 3(a) and 3(b)], the larger the control effect $\Delta\kappa$. This result is consistent with our previous work,[24] which discusses the influence of noise in the collapse and recovery processes. Simulation results for $\Delta\kappa$ vs L of controlled species in empirical networks B, C, and D are in Appendix C of the supplementary material.

In summary, the deterministic dynamic mechanism by which the collapse tipping point occurs is a reverse saddle-node bifurcation at κ_c as the value of κ increases as seen in Fig. 4. When the value of κ decreases, the recovery tipping point occurs in a saddle-node bifurcation at κ_r. Since $\kappa_r < \kappa_c$, hysteresis occurs in which the environment has to improve substantially of the system to recover as seen in Fig. 5.[1] Noise of different strengths affects the tipping point in both processes; thus, the control required to achieve the desired effect is different for systems perturbed by different noise strengths, which means that the individual species to be controlled change the tipping point differently. According to the analysis in previous works,[1,14,24] when the value of κ decreases, the parameter change or distance that needs to be overcome for the system to make the transition to the survival state is smaller. Then, the noise can help the system to make the transition. From a previous analysis,[14] as the value of κ increases, greater is the distance that the system has to overcome to escape from a low-abundance steady state to a high-abundance steady state. In this case, a combination of control and noise can accomplish the recovery. For a larger distance, it is necessary to control the decay rate of the pollinators, perhaps having more mutualistic links and a larger noise strength. When we combine the two, there is a relationship shown in Fig. 6 between the strength of the noise perturbation for both collapse and recovery. For the collapse process, demographic noise has a dominant effect, while for the recovery, it is the environmental noise.[24] We have performed calculations for empirical networks, random networks, and scale-free networks, shown in Figs. 6(a)–6(c), respectively, and find that this conclusion applies universally to all three kinds of networks.

C. Control effects for different network structures

We address the issue of nestedness by comparing the recovery dynamics of empirical stochastic mutualistic networks. Recent studies suggested[24] that, as networks become more nested, the values of collapse tipping point parameters become larger.[14] Thus, we study the control effect when different nesting is assumed. As shown in Fig. 7, the relationship between the control effect and the mutualistic number possessed by the controlled species in the random

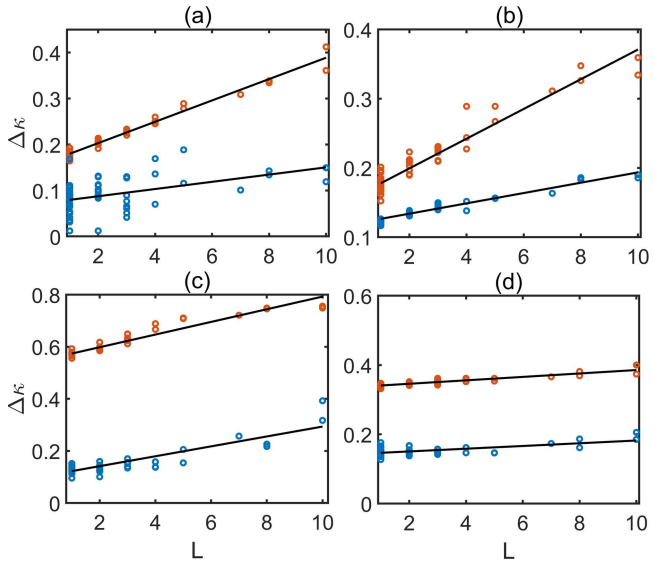

FIG. 3. Quantitative relationships between control effects and control species for the empirical stochastic mutualistic network A. (a) and (b) represent the recovery process and the collapse process with environmental noise, respectively. The brown dots and its fitted line represent the noise strength $\sigma = 0.1$, and blue dots and its fitted line correspond to $\sigma = 0.001$. (c) and (d) are the recovery process and the collapse process with demographic noise. The brown dots and its fitted line represent the noise strength $\xi = 0.25$, and blue dots and its fitted line correspond to $\xi = 0.1$. The parameter values of the network A are $\alpha_i^{(X)} = \alpha_i^{(Y)} = 0.3$, $\beta_{ii}^{(X)} = \beta_{ii}^{(Y)} = 1$, $\gamma = 1$, $h = 0.2$, $\rho = 0.5$, $\mu_X = 10^{-4}$, and $\mu_Y = 10^{-4}$. Each simulation has been calculated for $T = 400$, enough to allow species abundances to make the transition to another stable state. The initial conditions are randomly chosen in the basin of a high-abundance steady state for the collapse process and in the basin of a low-abundance steady state for the recovery process. There are a number of pollinators in the empirical network that have the same mutualistic numbers, but they are not all associated with the same plants; therefore, some of the dots vary for the same mutualistic numbers.

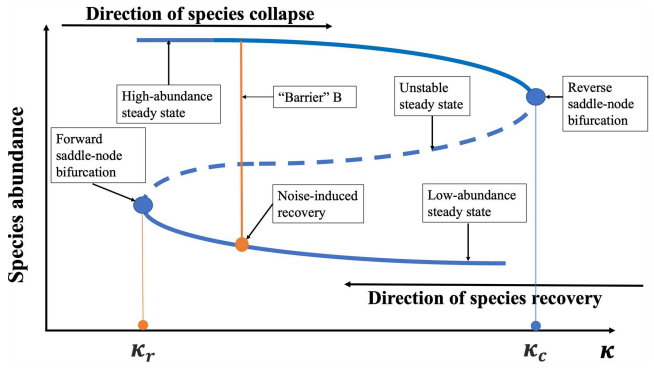

FIG. 4. A schematic illustration of the dynamical mechanisms of the noise induced collapse and recovery processes. The deterministic threshold corresponds to the occurrence of the reverse saddle-node bifurcation, and the backward recovery process is the result of the reverse saddle-node bifurcation.

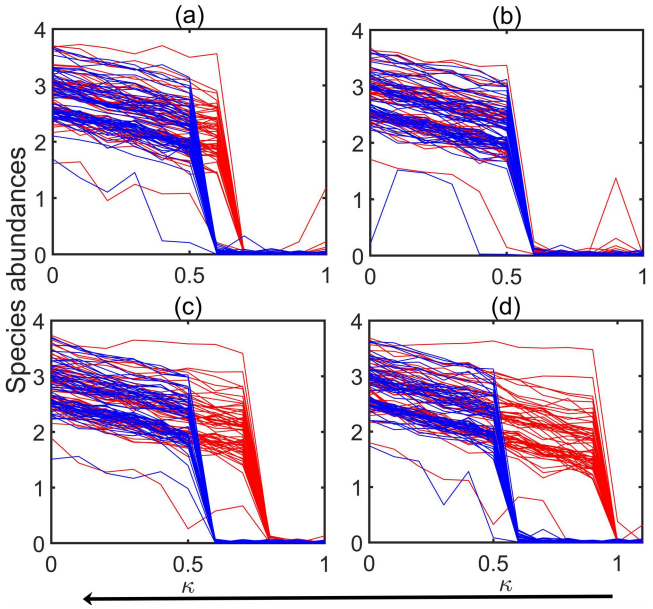

FIG. 5. A comparison of the collapse process and the recovery process with or without noise perturbations. (a) and (b) represent the collapse and recovery processes with the environmental noise with the strength of $\sigma = 0.1$, respectively. (c) and (d) represent the collapse and recovery processes with the demographic noise with the strength of $\zeta = 1$, respectively. All the blue curves represent the transition without noise disturbance, and the red curves represent the transition disturbed by noise. Environmental noise changes the tipping point very significantly during recovery and not so much during collapse.

network is consistent with the relationship obtained for the empirical networks. The results for other nestedess values are presented in Appendix C of the supplementary material.

The scale-free network also provides a good description of the growth and preferential attachment properties of real-world networks. Scale-free networks have hubs with a large number of connections. The distribution of connections between nodes follows a power law, signifying a high degree of nestedness, where most of the nodes have only a few connections, while a few nodes have a large number of connections. As shown in Fig. 7, the scale-free mutualistic network also follows the principle that the control effect is positively correlated with the mutualistic numbers of the controlled species.

The value of the control effect $\Delta\kappa$ is not the same for different networks. For example, the value of the control effect in the empirical network A is generally smaller than the value of the control effect in the random network. This is caused by the network structure. The empirical network A, as shown in Fig. 3(a), is affected by environmental noise $\sigma = 0.1$. The species with the greatest mutualistic numbers has $L_A = 10$, which corresponds to the control effect of $\Delta\kappa = 0.4$. Whereas in the scale-free network A of Fig. 7(a) subjected to environmental noise $\sigma = 0.1$, the species with the highest mutualistic numbers has $L_s = 12$, which corresponds to a control effect of $\Delta\kappa = 0.8$. Under the same conditions, the control effect of controlling the species with a large mutualistic numbers, $L_r = 15$, of the

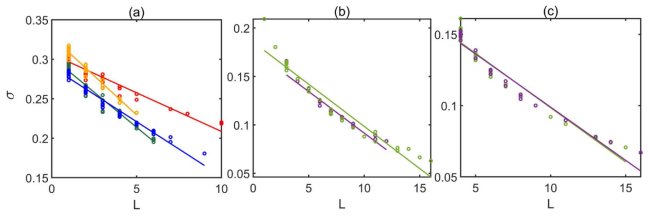

FIG. 6. *The relationship of noise disturbance and controlling effects.* (a), (b), and (c) present empirical networks, random networks, and scale-free networks, respectively. The red dots and its fitted line in (a) are network A, green dots and its fitted line are network B, blue dots and its fitted line are network C, and orange dots and its fitted line are network D. The green dots and its fitted line in (b) are random networks when *nestedness* = 0.3, and the purple dots and its fitted lines are random networks when *nestedness* = 0.5. The green dots and its fitted line in (c) are scale-free networks when *links probability* = 0.4, and purple dots and its fitted line are *links probability* = 0.6. Because we consider to control the decay rate of species with larger mutualistic links, the system has a transition with a smaller noise strength σ. We adjust the κ value of the uncontrolled species to the one before the system did not recover. The smaller the number of mutualistic species controlled, the larger the noise disturbance required for system transitions.

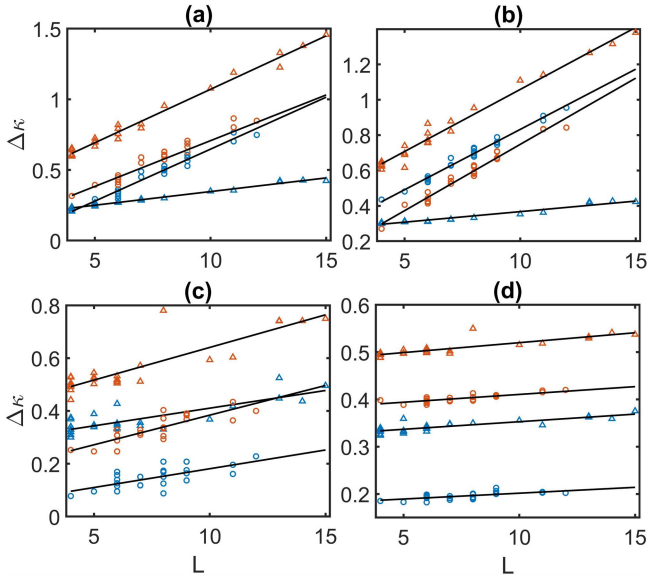

FIG. 7. Quantitative relationships between control effects and control species for the random mutualistic network A whose nestedness is 0.2 and the scale-free network whose links probability is 0.4. (a) and (b) represent the recovery process and the collapse process with environmental noise, respectively. The brown circle dots and its fitted line represent the noise strength $\sigma = 0.1$, and blue circle dots and its fitted line correspond to $\sigma = 0.001$ for the random network. (c) and (d) are the recovery process and the collapse process with demographic noise. The blue circle dots and its fitted line represent the noise strength $\xi = 0.1$, and brown circle dots and its fitted line correspond to $\xi = 0.25$ for the random network. The brown triangle dots and its fitted line represent the noise strength $\sigma = 0.1$, and blue triangle dots and its fitted line correspond to $\sigma = 0.001$ for the scale-free network. (c) and (d) are the recovery process and the collapse process with demographic noise. The blue triangle dots and its fitted line represent the noise strength $\xi = 0.1$, and brown triangle dots and its fitted line correspond to $\xi = 0.25$ for the scale-free network. The parameter values of the network A are $\alpha_i^{(X)} = \alpha_i^{(Y)} = 0.3$, $\beta_{ij}^{(X)} = \beta_{ij}^{(Y)} = 1$, $\gamma = 1$, $h = 0.2$, $\rho = 0.5$, $\mu_X = 10^{-4}$, and $\mu_Y = 10^{-4}$. The values of nestedness is 0.2. Each simulation has been calculated for $T = 400$, enough to allow the mutualistic species abundances to make a transition to another stable state. The initial conditions are randomly chosen in the basin of a high-abundance steady state for the collapse process and in the basin of a low-abundance steady state for the recovery process.

random network A is $\Delta\kappa = 1.5$. We compare the mutualistic numbers for each pollinator and their ranking for the three networks in Fig. 8(a). Pollinators in the empirical network contain fewer mutualistic plants than pollinators in the random and scale-free networks, and the empirical network is also less effective than the other two networks in controlling equally ranked pollinators. For example, when controlling the first ranked species of the three networks, the empirical network has a smaller value of control effect $\Delta\kappa$ than the random and scale-free networks. In the random network that we generated, most of the pollinators have the same number (4–6) of mutualistic plants. In the scale-free network, the number of pollinators with large mutualistic numbers is small, with the majority of pollinators having between four and six mutualistic plants, less than half the number of pollinators with large mutualistic numbers. The combinations of other empirical, random, and scale-free networks can be seen in Fig. 8.

A previous work[1,2] addressed the increase in the value of $\langle\gamma_x\rangle$ and $\langle\gamma_y\rangle$ to promote controllability. A greater strength of a mutualistic interaction is also associated with a greater mutual influence between species in the network. Since the mutualistic interaction is very complex and varies from species to species, we use the reduced model[29] to quantify the complex stochastic dynamics. $\langle\gamma_x\rangle$ and $\langle\gamma_y\rangle$ denote the simplified $\gamma_{ij}^{(X)}$ and $\gamma_{ij}^{(Y)}$, respectively, written as[29]

$$\langle\gamma_x\rangle = \frac{\sum_{i=1}^{S_X} \gamma N_{X_i}^{1-t} \times N_{X_i}}{\sum_{i=1}^{S_X} N_{X_i}}, \tag{7}$$

$$\langle\gamma_y\rangle = \frac{\sum_{i=1}^{S_Y} \gamma N_{Y_i}^{1-t} \times N_{Y_i}}{\sum_{i=1}^{S_Y} N_{Y_i}}, \tag{8}$$

where N_{X_i} and N_{Y_i} are the numbers of mutualistic interaction links relevant to X_i and Y_i in the full network. The ranking of pollinators and plants is calculated based on the eigenvectors of maximum eigenvalues associated with the respective projection networks.[1]

The projection matrices of pollinators and plants are expressed as $M_x = M^T \times M$ and $M_y = M^T \times M$, respectively. M is the $m \times n$ matrix that describes the original binary network, and m and n are numbers of pollinators and plants, respectively, and V_X and V_Y are components of the eigenvector corresponding to the maximum eigenvalues of M_X and M_Y, respectively. Then, we obtain

$$\langle\gamma_x\rangle = \frac{\sum_{i=1}^{S_X} \gamma N_{X_i}^{1-t} \times V_{X_i}}{\sum_{i=1}^{S_X} V_{X_i}}, \tag{9}$$

$$\langle\gamma_y\rangle = \frac{\sum_{i=1}^{S_Y} \gamma N_{Y_i}^{1-t} \times V_{Y_i}}{\sum_{i=1}^{S_Y} V_{Y_i}}. \tag{10}$$

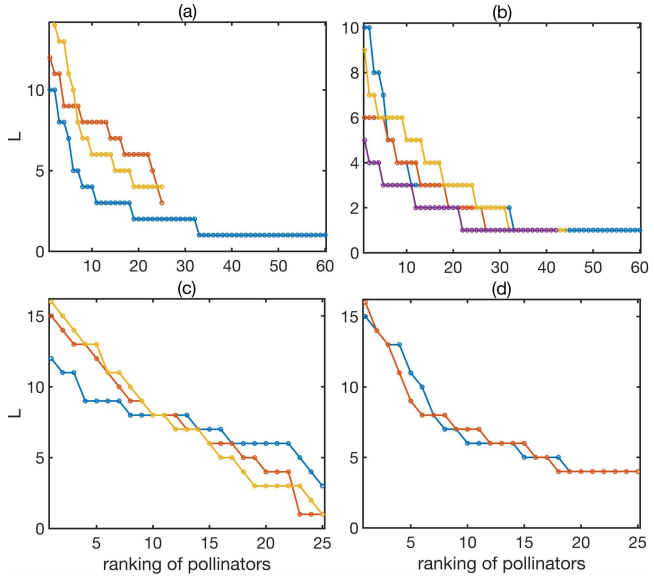

FIG. 8. Comparison of pollinators ranking among three types of networks. The blue, red, and yellow data points in (a) represent empirical A, random, and scale-free networks, respectively. (b), (c), and (d) present empirical networks, random networks, and scale-free networks, respectively. For pollinators with the same ranking, the pollinators of the empirical network corresponded to the lowest number of mutualistic plants. In the three networks, some of the different pollinators had the same mutualistic numbers, and we labeled them as ranked side-by-side, after which the species were then ranked sequentially. There were 61 pollinators in empirical network A and 25 pollinators in both the random and scale-free networks.

According to the above proposed procedure, we obtain that the mutualistic interaction strengths of the empirical network A are $\langle\gamma_x\rangle = 1.70$ and $\langle\gamma_y\rangle = 2.21$, the mutualistic interaction strengths of the random network are $\langle\gamma_x\rangle = 2.83$ and $\langle\gamma_y\rangle = 2.85$, and for the scale-free network are $\langle\gamma_x\rangle = 2.83$ and $\langle\gamma_y\rangle = 2.83$. The values of mutualistic numbers of both the random network and the scale-free network are greater than that of the empirical network A. The scale-free structure shows that the control of a single hub species is more pronounced since more species are affected by that species. Our argument based on random networks and scale-free networks applies to other empirical networks.

The control effect results in a stochastic complex network also confirms the universal property of linear and nonlinear control—the *importance* of node control. In linear node control, importance is the probability that the node appears in the minimum control set. In our study of nonlinear node control, importance is defined as the ability of the node to return to the survival state after the system experiences a sudden collapse at the tipping point. According to previous studies, nonlinear and linear node control importance in the network shows an opposite trend;[2] i.e., the large degree nodes in the network tend to be more important for nonlinear node control importance, while the small degree nodes are more dominant for linear node control importance. Our study shows that even in stochastic complex networks, controlling larger degree nodes has still larger importance than smaller degree nodes, but larger noise intensities can affect the control effect.

IV. THEORETICAL UNDERSTANDING OF THE QUANTITATIVE RELATION

Based on the nonlinear dynamics described in Fig. 4, B is the barrier height that the system must overcome to recover with the help of noise. The barrier height B depends on the value of κ. To explore the proportional relationship between B and κ, we perform a stability analysis of the reduced model[29] of the full high-dimensional model (see Appendix A of the supplementary material), yielding an algebraic relationship between pollinator and plant abundances and κ. Figure 9 shows the numerical solution of the reduced model showing the barrier height dependence of pollinators B_x and plants B_y on κ as both are proportional to $\Delta\kappa_r$, where $\Delta\kappa_r = |\kappa - \kappa_r|$. Under the influence of additive Gaussian distributed white noise, this scale happens in principle for any small noise amplitude for large time. In order for the system to recover in a finite time, the probability of noise disturbance needs to exceed B. For additive white environmental noise, this probability is expressed as[14,45]

$$P = \frac{1}{\sqrt{2\pi}\sigma}\int_P^\infty \exp\left(-\frac{x^2}{2\sigma^2}\right)dx = \frac{1}{2}erfc(cB), \tag{11}$$

where $erfc(.)$ is the complementary error function and $c = \frac{1}{\sqrt{2}\sigma}$. The error function can be rewritten as[14]

$$erfc(x) \geq \frac{1}{2}\sqrt{\frac{2e}{\pi}}\frac{\sqrt{\phi-1}}{\phi}e^{-\phi x^2}, \tag{12}$$

where $\phi > 1$ is a constant, and then,

$$\frac{1}{2}\sqrt{\frac{2e}{\pi}}\frac{\sqrt{\phi-1}}{\phi}e^{-\phi(cB)^2} \lesssim P \tag{13}$$

or

$$e^{-\phi(cB)^2} \gtrsim \sqrt{\frac{2\pi}{e}}\frac{\phi}{\sqrt{\phi-1}}P. \tag{14}$$

This gives

$$(cB)^2 \gtrsim \left|\ln\left(\sqrt{\frac{2\pi}{e}}\frac{\phi}{\sqrt{\phi-1}}P\right)\right|. \tag{15}$$

Since $c = \frac{1}{\sqrt{2}\sigma}$, then Eq. (15) is rewritten as

$$\left(\frac{B}{\sqrt{2}\sigma}\right)^2 \gtrsim \left|\ln\left(\sqrt{\frac{2\pi}{e}}\frac{\phi}{\sqrt{\phi-1}}P\right)\right| \tag{16}$$

or

$$\frac{B}{\sigma} \gtrsim \sqrt{2\left|\ln\left(\sqrt{\frac{2\pi}{e}}\frac{\phi}{\sqrt{\phi-1}}P\right)\right|}. \tag{17}$$

The right-hand side of Eq. (17) is greater than or equal to zero since P is greater than or equal to zero.

From the previous explanation, the value of B is determined by the value of $\Delta\kappa_r$. In order to investigate the specific relationship between B and $\Delta\kappa_r = |\kappa - \kappa_r|$, we calculate the algebraic relationship using the reduced model. From Fig. 9, we obtain that there

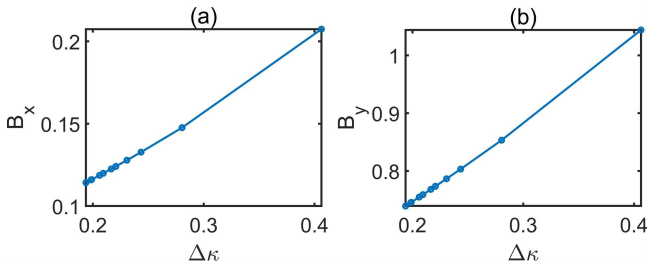

FIG. 9. The quantitative relationship of B and $\Delta\kappa$. B_x and B_y shown in (a) and (b), respectively, are associated with the unstable steady state solutions with the value of κ_p above the tipping point value, indicating a very clear positive correlation.

is a positive correlation $B \sim \Delta\kappa_r$ between B and $\Delta\kappa$. Substituting $B \sim \Delta\kappa_r$ into Eq. (17), we have

$$\Delta\kappa \gtrsim \sigma \sqrt{2\left|\ln\left(\sqrt{\frac{2\pi}{e}}\frac{\phi}{\sqrt{\phi-1}}P\right)\right|}, \tag{18}$$

from which it yields $\Delta\kappa \sim \sigma$.

V. DISCUSSION AND CONCLUSIONS

The control of ecological networks is an important topic for species survivability and habitat management. We investigate the role of controlling the decay rate of single or multiple pollinator species in a stochastic mutualistic complex network system in order to alter the collapse and recovery processes of the entire system. We particularly study the influence of noises, environmental and demographic, on the control of species abundances. Mutualistic interaction networks, due to their mutualistic properties, allow different species in the network to reach a mutually viable state of coexistence. In particular, even if most of the species are close to extinction, as long as one of the species with which they have mutualistic relationships survives, they can in principle survive. In this work, controlling the decay rate of a single pollinator or multiple pollinators means keeping the abundance of that pollinator or pollinators within a defined viable range. Plants that have mutualistic relationship with it or with them can use that relationship to survive. This in turn increases the survival rate of pollinators that are in a mutualistic relationship with those plants and are on the verge of extinction. We focus on how to control tipping points in ecological networks, including the relationship between the control method and the topological structure of the networks and under the influence of environmental and demographic noises.

The mutualistic complex network is a bipartite, high-dimensional ODE model representing pollinators and plants. The tipping point corresponds to saddle-node bifurcations in the system, exhibiting multistability[46–51] as the system parameters vary. In our case, it is a bistable system, as the two steady states with their own basins correspond to the survival state, in which all species coexist, and the extinction state, in which coexistence does occur. The unstable state between the basins of the survival state and the extinction state designates the basin boundary separating the two stable steady states.[43,52–57] There are two possibilities for a system to achieve a transition between two steady states. The first is through a change in the system parameters within the system. The second way is noise. For example, during the collapse process, the system can break through the basin of the extinction state across the unstable state and successfully transition to the survival state with the support of the noise.

In summary, in this work, we investigate the following: (1) A quantitative relationship between control effects and the controllability of the pollinator species being controlled based on empirical networks, random networks, and scale-free networks. (2) We analyze how noise perturbations affect the control effects and how to adjust the control strategies in the presence of noise disturbances. (3) We investigate the dependence of the topological structure of the networks on control effects. The results provide a controlling method for ecological systems with stochastic perturbations.

In ecosystems, controlling pollinators is more realistic than controlling plants. First, the more pollinators species are available, the more plants have the opportunity to benefit from the pollinators, the greater the abundances of plant species that result by the widespread presence of pollinators. Second, pollinators are more likely than plants to be intervened by external means, such as artificial breeding and the introduction of new species. Third, pollinators have a greater mobility and capacity for reproduction than plants. Finally, the introduction in a habitat of pollinators that are insensitive to environmental deterioration and that are in mutualistic relationships with the ones already in the habitat presents as a realistic ecological management control. Besides the interactions with pollinators, artificially interfering with plant abundances is also an issue for future discussions. For example, artificial breeding of highly resistant plants is used to stimulate the growth rate of the pollinators, which is also a very effective way of controlling and protecting ecosystems.

SUPPLEMENTARY MATERIAL

See the supplementary material for (i) the steady state solutions and the stability analysis based on the reduced model, (ii) simulation methods of the stochastic model, and (iii) numerical simulations for empirical mutualistic networks B–D, random networks B and C, and the scale-free network B.

ACKNOWLEDGMENTS

Y.M. was partially supported by the University of Aberdeen Elphinstone Fellowship.

DATA AVAILABILITY

The data that support the findings of this study are available from the corresponding author upon reasonable request.

REFERENCES

[1]J. Jiang, A. Hastings, and Y.-C. Lai, "Harnessing tipping points in complex ecological networks," J. R. Soc. Interface **16**, 20190345 (2019).
[2]J. Jiang and Y.-C. Lai, "Irrelevance of linear controllability to nonlinear dynamical networks," Nat. Commun. **10**, 1 (2019).

[3]L.-Z. Wang, R.-Q. Su, Z.-G. Huang, X. Wang, W.-X. Wang, C. Grebogi, and Y.-C. Lai, "A geometrical approach to control and controllability of nonlinear dynamical networks," Nat. Commun. **7**, 11323 (2016).
[4]Y.-Z. Sun, S.-Y. Leng, Y.-C. Lai, C. Grebogi, and W. Lin, "Closed-loop control of complex networks: A trade-off between time and energy," Phys. Rev. Lett. **119**, 198301 (2017).
[5]G. Yan, P. E. Vértes, E. K. Towlson, Y. L. Chew, D. S. Walker, W. R. Schafer, and A.-L. Barabási, "Network control principles predict neuron function in the *Caenorhabditis elegans* connectome," Nature **550**, 519 (2017).
[6]Y.-Z. Chen, L.-Z. Wang, W.-X. Wang, and Y.-C. Lai, "Energy scaling and reduction in controlling complex networks," R. Soc. Open Sci. **3**, 160064 (2016).
[7]X. F. Wang and G. Chen, "Pinning control of scale-free dynamical networks," Physica A **310**, 521–531 (2002).
[8]J. G. T. Zañudo, G. Yang, and R. Albert, "Structure-based control of complex networks with nonlinear dynamics," Proc. Natl. Acad. Sci. U.S.A. **114**, 7234–7239 (2017).
[9]C. Wang, C. Grebogi, and M. S. Baptista, "Nonlocality in complex networks," Chaos **26**, 093119 (2016).
[10]K. Tian, C. Bai, H.-P. Ren, and C. Grebogi, "Hyperchaos synchronization using univariate impulse control," Phys. Rev. E **100**, 052215 (2019).
[11]H.-P. Ren, Y. Yang, M. S. Baptista, and C. Grebogi, "Tumour chemotherapy strategy based on impulse control theory," Philos. Trans. R. Soc. A **375**, 20160221 (2017).
[12]M. Chiang, S. H. Low, A. R. Calderbank, and J. C. Doyle, "Layering as optimization decomposition: A mathematical theory of network architectures," Proc. IEEE **95**, 255–312 (2007).
[13]L. Marucci, D. A. Barton, I. Cantone, M. A. Ricci, M. P. Cosma, S. Santini, D. di Bernardo, and M. di Bernardo, "How to turn a genetic circuit into a synthetic tunable oscillator, or a bistable switch," PLoS One **4**, e8083 (2009).
[14]Y. Meng, J. Jiang, C. Grebogi, and Y.-C. Lai, "Noise-enabled species recovery in the aftermath of a tipping point," Phys. Rev. E **101**, 012206 (2020).
[15]A. Hastings, K. C. Abbott, K. Cuddington, T. Francis, G. Gellner, Y.-C. Lai, A. Morozov, S. Petrovskii, K. Scranton, and M. L. Zeeman, "Transient phenomena in ecology," Science **361**, eaat6412 (2018).
[16]J. Roughgarden, "A simple model for population dynamics in stochastic environments," Am. Nat. **109**, 713–736 (1975).
[17]R. Lande, "Risks of population extinction from demographic and environmental stochasticity and random catastrophes," Am. Nat. **142**, 911–927 (1993).
[18]R. Lande, "Demographic stochasticity and Allee effect on a scale with isotropic noise," Oikos **83**, 353–358 (1998).
[19]J. Ripa, P. Lundberg, and V. Kaitala, "A general theory of environmental noise in ecological food webs," Am. Nat. **151**, 256–263 (1998).
[20]M. B. Bonsall and A. Hastings, "Demographic and environmental stochasticity in predator–prey metapopulation dynamics," J. Anim. Ecol. **73**, 1043–1055 (2004).
[21]B. Dennis, "Allee effects in stochastic populations," Oikos **96**, 389–401 (2002).
[22]Y.-C. Lai, "Beneficial role of noise in promoting species diversity through stochastic resonance," Phys. Rev. E **72**, 042901 (2005).
[23]O. N. Bjørnstad, "Nonlinearity and chaos in ecological dynamics revisited," Proc. Natl. Acad. Sci. U.S.A. **112**, 6252–6253 (2015).
[24]Y. Meng, Y.-C. Lai, and C. Grebogi, "Tipping point and noise-induced transients in ecological networks," J. R. Soc. Interface **17**, 20200645 (2020).
[25]J. L. Bronstein, *Mutualism* (Oxford University Press, New York, 2015).
[26]P. P. Staniczenko, J. C. Kopp, and S. Allesina, "The ghost of nestedness in ecological networks," Nat. Commun. **4**, 1391 (2013).
[27]R. P. Rohr, S. Saavedra, and J. Bascompte, "On the structural stability of mutualistic systems," Science **345**, 1253497 (2014).
[28]J. J. Lever, E. H. Nes, M. Scheffer, and J. Bascompte, "The sudden collapse of pollinator communities," Ecol. Lett. **17**, 350–359 (2014).
[29]J. Jiang, Z.-G. Huang, T. P. Seager, W. Lin, C. Grebogi, A. Hastings, and Y.-C. Lai, "Predicting tipping points in mutualistic networks through dimension reduction," Proc. Natl. Acad. Sci. U.S.A. **115**, E639–E647 (2018).
[30]B. Walker, C. S. Holling, S. R. Carpenter, and A. Kinzig, "Resilience, adaptability and transformability in social–ecological systems," Ecol. Soc. **9**, 5 (2004).
[31]C. S. Holling, "Resilience and stability of ecological systems," Annu. Rev. Ecol. Syst. **4**, 1–23 (1973).
[32]C. S. Holling, "Some characteristics of simple types of predation and parasitism," Can. Entomol. **91**, 385–398 (1959).
[33]S. R. Carpenter, J. J. Cole, M. L. Pace, R. Batt, W. A. Brock, T. Cline, J. Coloso, J. R. Hodgson, J. F. Kitchell, D. A. Seekell, L. Smith, and B. Weidel, "Early warnings of regime shifts: A whole-ecosystem experiment," Science **332**, 1079–1082 (2011).
[34]C. Boettiger and A. Hastings, "Quantifying limits to detection of early warning for critical transitions," J. R. Soc. Interface **9**, 2527–2539 (2012).
[35]A. Hastings, "Timescales and the management of ecological systems," Proc. Natl. Acad. Sci. U.S.A. **113**, 14568–14573 (2016).
[36]J. M. Drake and B. D. Griffen, "Early warning signals of extinction in deteriorating environments," Nature **467**, 456–459 (2010).
[37]A. Morozov, K. C. Abbott, K. Cuddington, T. Francis, G. Gellner, A. Hastings, Y.-C. Lai, S. Petrovskii, K. Scranton, and M. L. Zeeman, "Long transients in ecology: Theory and applications," Phys. Life Rev. **32**, 1–40 (2020).
[38]C. Grebogi, "Sudden regime shifts after apparent stasis. Comment on 'Long transients in ecology: Theory and applications' by Andrew Morozov *et al.*," Phys. Life Rev. **32**, 41–43 (2020).
[39]C. Boettiger and A. Hastings, "Tipping points: From patterns to predictions," Nature **493**, 157–158 (2013).
[40]V. Dakos and J. Bascompte, "Critical slowing down as early warning for the onset of collapse in mutualistic communities," Proc. Natl. Acad. Sci. U.S.A. **111**, 17546–17551 (2014).
[41]J. T. Kerr, A. Pindar, P. Galpern, L. Packer, S. G. Potts, S. M. Roberts, P. Rasmont, O. Schweiger, S. R. Colla, L. L. Richardson *et al.*, Climate change impacts on bumblebees converge across continents," Science **349**, 177–180 (2015).
[42]Y. L. Dupont, D. M. Hansen, and J. M. Olesen, "Structure of a plant–flower-visitor network in the high-altitude sub-alpine desert of Tenerife, Canary Islands," Ecography **26**, 301–310 (2003).
[43]S. Balaji, M. M. Babu, L. M. Iyer, N. M. Luscombe, and L. Aravind, "Comprehensive analysis of combinatorial regulation using the transcriptional regulatory network of yeast," J. Mol. Biol. **360**, 213–227 (2006).
[44]J. J. Lever, E. H. van Nes, M. Scheffer, and J. Bascompte, "The sudden collapse of pollinator communities," Ecol. Lett. **17**, 350–359 (2014).
[45]S.-H. Chang, P. C. Cosman, and L. B. Milstein, "Chernoff-type bounds for the Gaussian error function," IEEE Trans. Commun. **59**, 2939–2944 (2011).
[46]U. Feudel and C. Grebogi, "Multistability and the control of complexity," Chaos **7**, 597–604 (1997).
[47]S. Kraut, U. Feudel, and C. Grebogi, "Preference of attractors in noisy multistable systems," Phys. Rev. E **59**, 5253–5260 (1999).
[48]S. Kraut and U. Feudel, "Multistability, noise, and attractor hopping: The crucial role of chaotic saddles," Phys. Rev. E **66**, 015207 (2002).
[49]U. Feudel and C. Grebogi, "Why are chaotic attractors rare in multistable systems?," Phys. Rev. Lett. **91**, 134102 (2003).
[50]A. N. Pisarchik and U. Feudel, "Control of multistability," Phys. Rep. **540**, 167–218 (2014).
[51]Y.-C. Lai and C. Grebogi, "Quasiperiodicity and suppression of multistability in nonlinear dynamical systems," Euro. Phys. J. Spec. Top. **226**, 1703–1719 (2017).
[52]Y.-C. Lai and T. Tél, *Transient Chaos—Complex Dynamics on Finite Time Scales* (Springer, New York, 2011).
[53]S. W. McDonald, C. Grebogi, E. Ott, and J. A. Yorke, "Fractal basin boundaries," Physica D **17**, 125–153 (1985).
[54]P. Hessari, Y. Do, Y.-C. Lai, J. Chae, C. W. Park, and G. Lee, "Regularization of chaos by noise in electrically driven nanowire systems," Phys. Rev. B **89**, 134304 (2014).
[55]R. M. May, "Biological populations with nonoverlapping generations: Stable points, stable cycles, and chaos," Science **186**, 645–647 (1974).
[56]A. Hastings, C. L. Hom, S. Ellner, P. Turchin, and H. C. J. Godfray, "Chaos in ecology: Is mother nature a strange attractor?," Annu. Rev. Ecol. Syst. **24**, 1–33 (1993).
[57]C. Grebogi, E. Ott, and J. A. Yorke, "Crises, sudden changes in chaotic attractors and chaotic transients," Physica D **7**, 181–200 (1983).